



Modeling A β 42 Accumulation in Response to Herpes Simplex Virus 1 Infection: Two Dimensional or Three Dimensional?

Eric E. Abrahamson,^{a,b} Wenxiao Zheng,^{c,d} Vaishali Muralidaran,^d Milos D. Ikonovic,^{a,b,d} David C. Bloom,^e Vishwajit L. Nimgaonkar,^{d,f}  Leonardo D'Aiuto^{d,f}

^aDepartment of Neurology, University of Pittsburgh School of Medicine, Pittsburgh, Pennsylvania, USA

^bGeriatric Research Education and Clinical Center, Pittsburgh VA Healthcare System, Pittsburgh, Pennsylvania, USA

^cDepartment of Psychiatry, The Second Xiangya Hospital, Xiangya School of Medicine, Central South University, Changsha, China

^dDepartment of Psychiatry, Western Psychiatric Institute and Clinic, University of Pittsburgh School of Medicine, Pittsburgh, Pennsylvania, USA

^eDepartment of Molecular Genetics & Microbiology, University of Florida College of Medicine, Gainesville, Florida, USA

^fVISN 4 MIRECC, VA Pittsburgh Healthcare System, Pittsburgh, Pennsylvania, USA

ABSTRACT Alzheimer's disease is a progressive neurodegenerative disease characterized neuropathologically by the presence of extracellular amyloid plaques composed of fibrillar amyloid beta (A β) peptides and intracellular neurofibrillary tangles. Postmortem and *in vivo* studies implicate herpes simplex virus 1 (HSV-1) infection in the brain as a precipitating factor in disease/pathology initiation. HSV-1 infection of two-dimensional (2D) neuronal cultures causes intracellular accumulation of A β 42 peptide, but these 2D models do not recapitulate the three-dimensional (3D) architecture of brain tissue. We employed human induced pluripotent stem cells (hiPSCs) to compare patterns of A β 42 accumulation in HSV-1-infected 2D (neuronal monolayers) and 3D neuronal cultures (brain organoids). Akin to prior studies, HSV-1-infected 2D cultures showed A β 42 immunoreactivity in cells expressing the HSV-1 antigen ICP4 (ICP4⁺). Conversely, accumulation of A β 42 in ICP4⁺ cells in infected organoids was rarely observed. These results highlight the importance of considering 3D cultures to model host-pathogen interaction.

IMPORTANCE The pathogen hypothesis of Alzheimer's disease (AD) proposes that brain HSV-1 infection is an initial source of amyloid beta (A β) peptide-containing amyloid plaque development. A β accumulation was reported in HSV-1-infected 2D neuronal cultures and neural stem cell cultures as well as in HSV-1-infected 3D neuronal culture models. The current study extends these findings by showing different patterns of A β 42 accumulation following HSV-1 infection of 2D compared to 3D neuronal cultures (brain organoids). Specifically, 2D neuronal cultures showed A β 42 immunoreactivity mainly in HSV-1-infected cells and only rarely in uninfected cells or infected cells exposed to antivirals. Conversely, 3D brain organoids showed accumulation of A β 42 mainly in noninfected cells surrounding HSV-1-infected cells. We suggest that because brain organoids better recapitulate architectural features of a developing brain than 2D cultures, they are a more suitable model to investigate the involvement of HSV-1 in the onset of AD pathology.

KEYWORDS Alzheimer's disease, brain organoids, herpes simplex virus 1, HSV-1, induced pluripotent stem cells, iPSCs

Alzheimer's disease (AD) is a leading cause of dementia, yet its etiology is unknown and there is no effective therapy to prevent or arrest the disease. Primary neuropathological lesions of AD are extracellular plaques of fibrillized amyloid- β (A β) peptides and intracellular neurofibrillary tangles of hyperphosphorylated tau (p-tau) protein (1). A β plaques develop early in AD and can influence tau phosphorylation (2) and

Citation Abrahamson EE, Zheng W, Muralidaran V, Ikonovic MD, Bloom DC, Nimgaonkar VL, D'Aiuto L. 2021. Modeling A β 42 accumulation in response to herpes simplex virus 1 infection: two dimensional or three dimensional? *J Virol* 95:e02219-20. <https://doi.org/10.1128/JVI.02219-20>.

Editor Rozanne M. Sandri-Goldin, University of California, Irvine

Copyright © 2021 Abrahamson et al. This is an open-access article distributed under the terms of the [Creative Commons Attribution 4.0 International license](https://creativecommons.org/licenses/by/4.0/).

Address correspondence to Leonardo D'Aiuto, daiutol@upmc.edu.

Received 17 November 2020

Accepted 17 November 2020

Accepted manuscript posted online 2 December 2020

Published 10 February 2021

neuroinflammation (3), two processes more closely tied to cognitive impairment (4). This series of events was formalized as the amyloid cascade hypothesis of AD (5). Involvement of infective pathogens in AD pathogenesis was first proposed by Alois Alzheimer (6) and is supported by several recent studies that suggested that A β is an antimicrobial peptide (AMP) that plays a role in protecting neurons from infectious pathogens like bacteria and viruses (7, 8). In this regard, increased A β production could be a protective response to infection but may lead to excessive A β accumulation and, possibly, fibrillization and deposition as amyloid plaques. Supporting this hypothesis, the neurotropic pathogen HSV-1 was detected in A β plaques in AD brains (9). *In vitro* studies using two-dimensional (2D) monolayer neuronal cultures reported that HSV-1 infection resulted in intracellular A β accumulation and upregulation of β -secretase and the nicastrin component of γ -secretase, which are required for the generation of A β from its precursor protein (10). This phenomenon could be due to intermittent cycles of HSV-1 reactivation in the brain (11). A recent study using an *in vitro* three-dimensional (3D) model of human brain also described extracellular accumulation of A β 42 following infection with HSV-1 (12), possibly due to HSV-1-induced A β overproduction/secretion and/or seeding of A β aggregation in the extracellular space by virus particles as an antimicrobial response (13). However, not well-understood are the mechanisms underlying altered A β production and accumulation during lytic HSV-1 infection or repeated cycles of viral reactivation and how HSV-1-infected cells communicate with nearby cells to initiate this response.

We have recently reported on the use of induced pluripotent stem cells (iPSCs) to model HSV-1 acute and latent infection in 2D monolayer neuronal cultures and 3D brain organoids (14). These *in vitro* models showed that iPSC-derived CNS neurons are permissive for HSV-1 infection, with reporter gene expression being detected from both immediate-early (ICP0) and strict late (gC) promoters and infectious virus being released into the medium during the acute infection period of both 2D and 3D cultures. In addition, we demonstrated that HSV-1 can establish latency in both culture systems. Perhaps the most novel finding of these studies was that 3D brain organoids, but not 2D monolayer neuronal cultures, have the ability to recapitulate the difficulty that HSV-1 has in reactivating from latency in the central nervous system (CNS), as observed in animal models (14). This ability contributes to the potential superiority of 3D brain organoids to model host-pathogen interactions within the CNS.

In this study, we employed iPSC-derived 2D monolayer neuronal cultures and 3D brain organoids to investigate the accumulation of A β 42 in response to HSV-1 infection. This investigation compared the relative amount of HSV-1-induced A β 42 in the two models following infection.

RESULTS

We initially investigated A β 42 accumulation in 2D neuronal cultures derived from human induced pluripotent stem cells (hiPSCs) and acutely infected at a multiplicity of infection (MOI) of HSV-1, strain KOS, of 1, 0.7, 0.5, and 0.3. To block productive viral replication, neurons infected at an MOI of 0.3 were also maintained in the presence of antivirals [(E)-5-(2-bromovinyl)-2'-deoxyuridine (5BVdU) and interferon alpha (IFN- α)]. The expression of an HSV-1 lytic gene, infected-cell polypeptide 4 (ICP4), and A β 42 in uninfected and infected cells was analyzed by immunocytochemistry (ICC) at 48 h postinfection (p.i.) (Fig. 1). Neurons in uninfected cultures showed faint, punctate A β 42 immunoreactivity surrounding the nucleus (Fig. 1a). When cultures were infected at an MOI of 0.3 with the antivirals 5BVdU and IFN- α , no increase in A β 42 immunoreactivity was observed, even in the rarely observed ICP4⁺ cells (Fig. 1b). When 2D cultures were infected with HSV-1 at MOIs of 1.0, 0.7, and 0.5, intense A β 42 immunoreactivity was observed in approximately 19% of ICP4⁺ cells but not in any of the uninfected cells in close proximity or distal to infected neurons (Fig. 1c and e). A β 42 immunoreactivity was observed surrounding and encapsulating the nucleus and consisted of dense

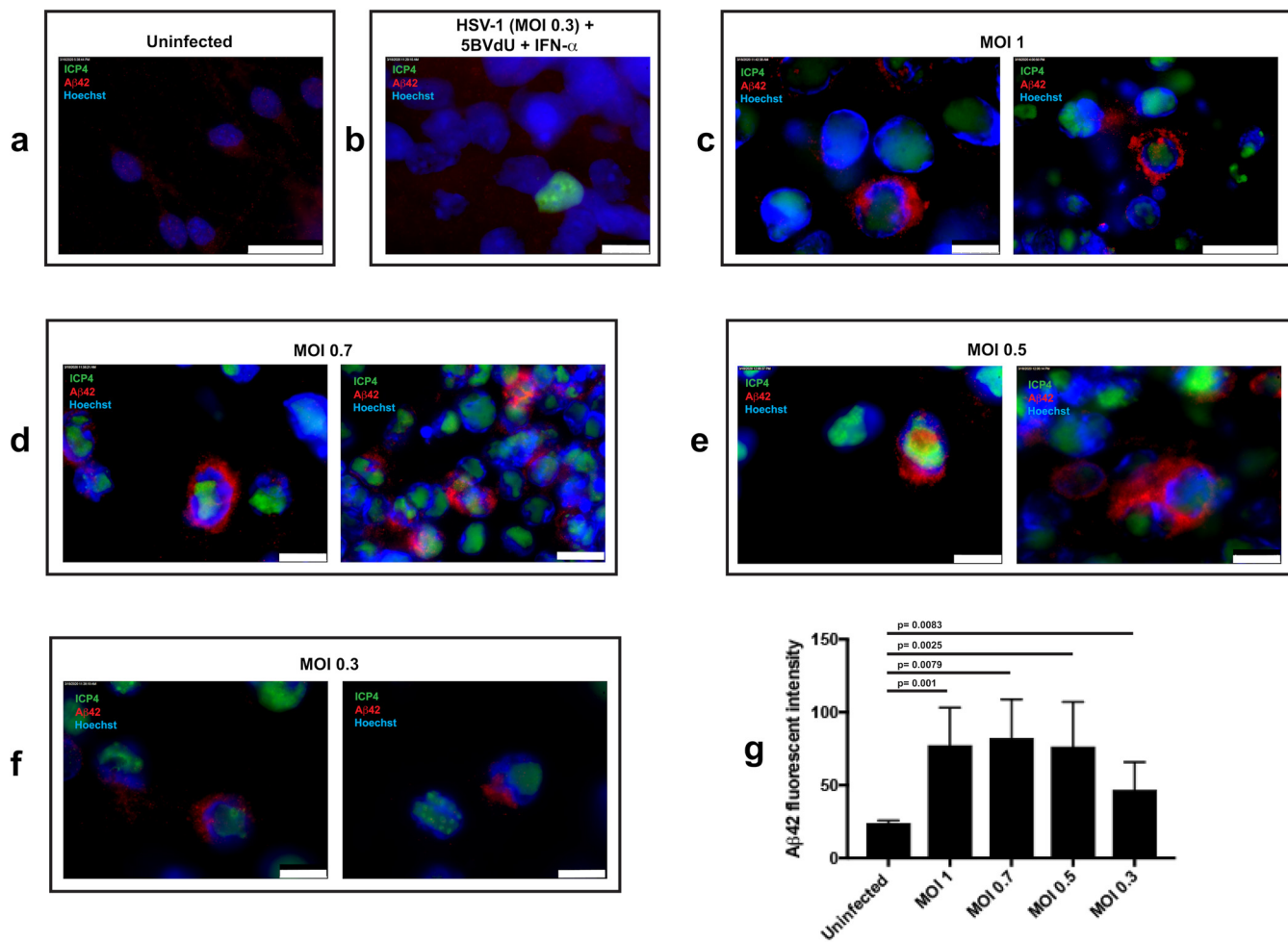


FIG 1 Immunofluorescence for amyloid- β 42 and the HSV-1 antigen ICP4 in uninfected and HSV-1-infected hiPSC-derived neurons. hiPSC-derived 2D neuronal cultures were infected at MOIs of 1 to 0.3. Neurons were also infected at an MOI of 0.3 in the presence of antivirals 5BVdU and IFN- α . (a to f) Microphotographs depicting immunostaining of A β 42 and the HSV-1 antigen ICP4 in uninfected neurons (a), neurons infected at an MOI of 0.3 in the presence of 5BVdU and IFN- α (b), and neurons acutely infected at MOIs of 1 to 0.3 (c to f). Scale bar is 25 μ m (a and c, right), 10 μ m (b; c, left; d; e; and f). Quantification of A β 42 immunofluorescence intensity using ImageJ (g). The increase in A β 42 fluorescence intensity in infected neurons compared to uninfected neurons was assessed using Student's *t* test. Error bars represent standard deviations.

puncta and larger globules of more dispersed A β 42 immunoreactivity. Similar patterns were observed at an MOI of 0.3 in approximately 8% of ICP4⁺ cells, although A β 42 immunoreactivity was less intense (Fig. 1f to g). These results, in line with other reports (10, 15), show that HSV-1 induces A β 42 accumulation in infected monolayer cultures of neurons and that antiviral treatment prevents this accumulation during this experimental time frame (Fig. 1b to f).

Next, we investigated the suitability of 3D neuronal cultures (i.e., brain cortical organoids) to model HSV-1-induced A β accumulation. Figure 2 illustrates the immunohistochemical characterization of a representative noninfected 3D brain organoid at 9 weeks *in vitro*. Cortical brain organoids were generated from hiPSC-derived neural rosettes (for details regarding the differentiation procedure and characterization, see the Materials and Methods).

Twelve-week-old organoids (~2-mm size) were infected singularly with HSV-1 strain KOS, using 3,000 PFU/organoid. The inocula were removed after 2 h, and organoids were analyzed at days 3 and 5 postinfection. A β accumulation was assessed by immunohistochemistry (IHC) analysis of sections obtained from formalin-fixed, paraffin-embedded organoids. IHC showed ICP4⁺ neurons throughout and up to ~250 μ m from the edge of the organoids (Fig. 3a). HSV-1-infected organoids exposed to the antivirals 5BVdU and IFN- α had no detectable ICP4⁺ cells (Fig. 3b), and A β 42

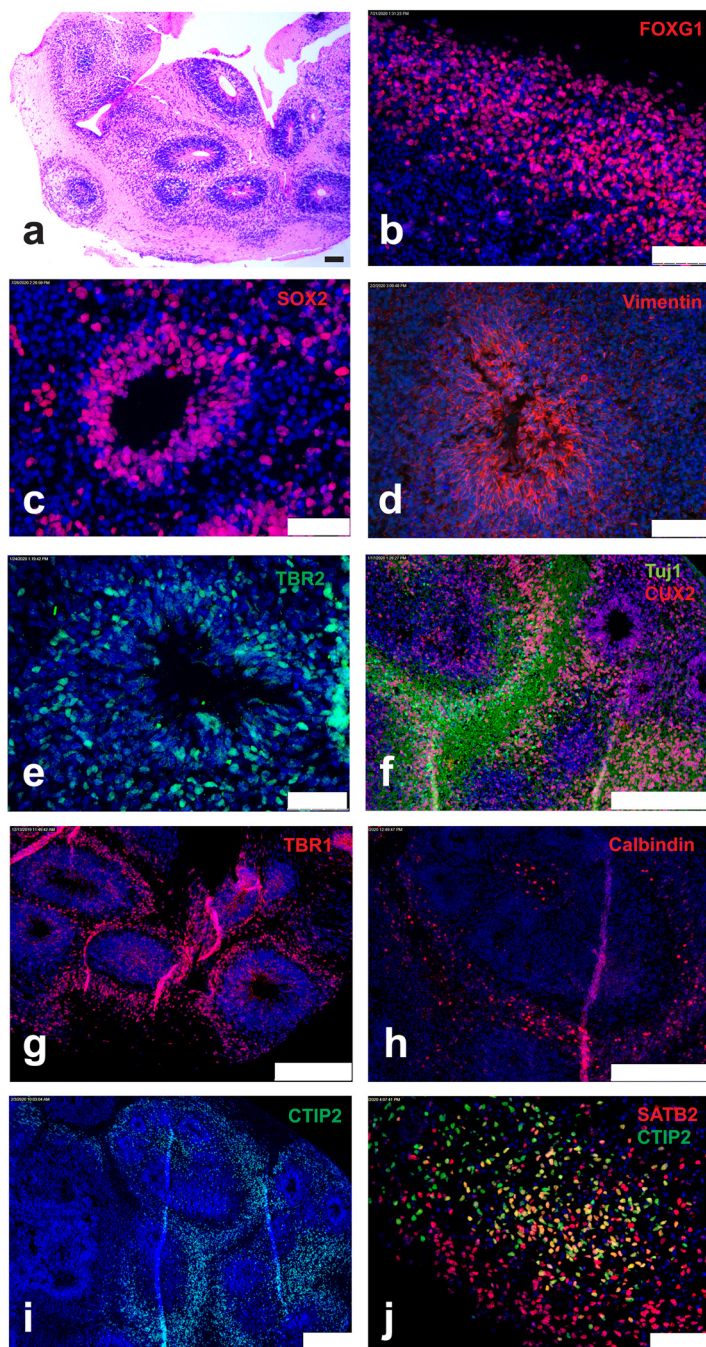


FIG 2 Characterization of 3D brain organoids. (a) Hematoxylin and eosin staining of 9-week-old organoids. (b to j) Immunostaining of 8- μ m-thick sections of organoids with antibodies recognizing FOXG1 (b), SOX2 (c), vimentin (d), TBR2 (e), Tuj/CUX2 (f), TBR1 (g), calbindin (h), CTIP2 (i), and CTIP2/SATB2 (j). Nuclei were counterstained with Hoechst 33342. Scale bars are 100 μ m (a), 75 μ m (b, d, and j), 50 μ m (c and e), and 250 μ m (f, g, h, and i).

immunoreactivity was comparable to that of uninfected organoids (Fig. 3c). Contrary to what was observed in infected 2D neuronal cultures, A β 42 immunoreactivity in ICP4⁺ cells was rarely observed in infected 3D organoids (Fig. 3d and e). In these rare instances, A β 42 immunoreactivity was observed mainly in areas that appeared to be between infected nuclei (Fig. 3d and e), and perinuclear punctate A β 42 immunoreactivity was not as robust as that in 2D cultures. In rare instances, A β 42 immunoreactivity overlapped ICP4⁺ particles (Fig. 3f). Colocalization of ICP4 with large areas of A β 42 immunoreactivity containing fragmented nuclei also was observed (Fig. 3g and h).

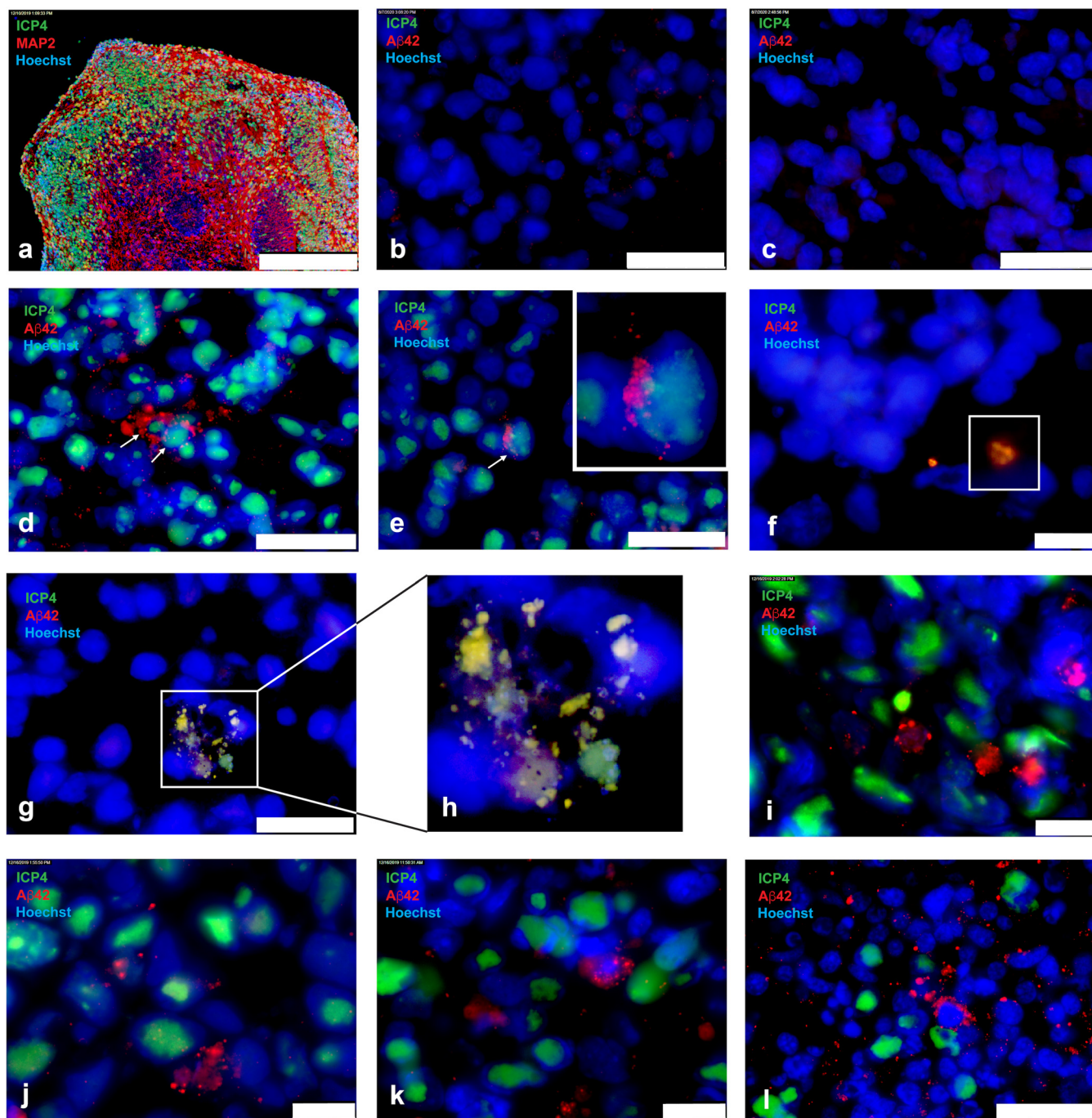


FIG 3 Immunofluorescence for amyloid- β 42 and the HSV-1 antigen ICP4 in uninfected and HSV-1-infected 3D brain organoids. Twelve-week-old organoids were infected singularly with 3,000 PFU in the presence or absence of antivirals 5BVDU and IFN- α . After 2 h, the inocula were removed and the organoids were cultured in the presence or absence of antivirals. After 72 h, the organoids were processed for immunofluorescence. (a) Microphotographs of 8- μ m-thick sections of HSV-1-infected (a) and uninfected (b) organoids immunostained with ICP4/MAP2 and infected organoids in the presence (c) or absence (d to l) of antivirals with ICP4/A β 42. Nuclei were counterstained with Hoechst 33342. ICP4⁺ cells exhibiting intracellular A β 42 immunoreactivity are indicated by arrows. The insets contain enlarged details. Scale bars are 250 μ m (a), 25 μ m (b, c, d, e, g, and i), and 10 μ m (f, i, j, and k).

Overall, in infected organoids, perinuclear A β 42 immunoreactivity was predominantly detected in ICP4⁻ cells surrounding ICP4⁺ infected cells (Fig. 3i to l). The robust perinuclear A β 42 immunoreactivity in ICP4⁻ cells resembled those observed in ICP4⁺ neurons in 2D cultures, and A β 42 was present between nuclei in extracellular spaces. These observations demonstrate that in the 3D brain organoid model (in contrast to 2D neuronal monolayers), A β 42 accumulates primarily in ICP4⁻ cells.

DISCUSSION

The pathogen hypothesis of AD posits that A β peptides are produced as a form of antimicrobial protection (AMP) in response to pathogens invading the CNS (10, 16, 17). Specifically, HSV-1 infection could be a trigger for persistent A β overproduction and A β plaque development (13), either alone or in combination with impaired A β clearance. A β exhibits antimicrobial properties (18) against a range of bacterial pathogens (19), influenza A virus (20), and herpesviruses (13), and its accumulation in AD may be a side effect of a host innate response to microbial invasion. Among the number of neurotropic viruses that infect the brain, HSV-1 in particular has been proposed as an initial source of A β plaque development (13). Recent studies have shown A β accumulation in HSV-1-infected 2D neuronal cultures and neural stem cell cultures, which could be interpreted as a mechanism initiated to prevent virus spread (21–24). A recent study provided evidence that A β exerts its AMP role by mediating viral agglutination (13). Based on these observations, the following questions emerge: how common is A β accumulation in HSV-1 infected cells, and is the 2D cell monolayer model the optimal choice for studying this phenomenon? Our current immunohistochemical analysis of HSV-1-infected 2D monolayer neuronal cultures showed high frequencies of perinuclear A β 42 immunoreactivity in ICP4⁺ cells compared to uninfected cells or infected cells exposed to antivirals 5BVdU and IFN- α . The frequency of ICP4⁺ cells exhibiting A β 42 immunoreactivity was progressively lowered by reducing the inoculum to an MOI of 0.3. These results support the ability of HSV-1 to trigger A β 42 accumulation. However, when we infected 3D brain organoids with HSV-1, A β 42 immunoreactivity exhibited a pattern distinct from that observed in 2D neuronal monolayers. Specifically, A β 42 immunoreactivity was observed primarily in ICP4⁻ neurons but rarely in ICP4⁺ neurons. A possible explanation for different patterns of A β 42 immunoreactivity in 2D monolayers versus 3D brain organoids is that the spread of infection and A β 42 production occurs at lower rates in the latter model, providing more translational value in studies of brain pathology. It is important to consider the possibility that antiviral factors produced in infected monolayer 2D neuronal cultures are diluted out in the culture medium, while within brain organoids, these factors reach at least the minimal concentration required to exert their antiviral activity. Furthermore, cell-to-cell communication, which is known to be impaired in 2D cultures (25), may contribute to the differences observed between these two *in vitro* systems. It is also important to consider that the ICP4⁻ cells that exhibit an increased A β 42 immunofluorescence may represent abortively infected cells rather than uninfected cells (26). A recent study by Drayman et al. on sorted cell populations to investigate HSV-1 infection at the single-cell level showed that antiviral response is initiated in ICP4⁻ cells (26). The antiviral genes IFIT1 and IFIT2 are specifically upregulated in the ICP4⁻ cells. In general, interferon-stimulated genes are more highly expressed in cells with low HSV-1 gene expression. Thus, it is possible that the increased A β 42 immunofluorescence we observed in ICP4-negative cells is the consequence of strong antiviral signaling elicited in this population of abortively infected cells. Though rarely detected in uninfected organoids, it is possible that a fraction of cells expressing A β 42 were present in organoids prior to HSV-1 infection and were ICP4⁻ due to the peptide's AMP activity.

In summary, we demonstrate that altered A β immunoreactivity due to HSV-1 infection differs in 3D brain organoids from that in 2D neuronal monolayers. In brain organoids, this response is associated with A β 42 immunoreactivity in ICP4⁻ cells. This differs from 2D monolayer cultures, where HSV-1 infection leads to A β 42 accumulation primarily in infected ICP4⁺ cells. Because 3D brain organoids of human iPSC recapitulate the 3D architecture of brain, they may be a more suitable model to study the interaction of neuronal HSV-1 infection or repeated cycles of viral reactivation with A β alterations in the context of a human neurodegenerative disease. Furthermore, brain organoids may provide critical insights into the mechanisms underlying the communication between HSV-1-infected cells and other cells in the same neuronal network, which can initiate A β pathology. Clarifying the role of HSV-1 in AD pathogenesis could lead to antiviral prophylactic or intervention trials, a novel approach supported by a

recent report of lower dementia risk associated with anti-herpetic medication for HSV-1 (27).

MATERIALS AND METHODS

Cell lines. Two hiPSC lines, 73-56010-01 SA and 73-56010-02, were employed in this study. Both hiPSC lines were generated from fibroblasts derived from skin biopsy samples that were collected from a healthy volunteer via 4-mm full-thickness punch biopsies under local anesthesia. All identifying information pertaining to the healthy volunteer was removed, and the hiPSCs were established at the National Institute of Mental Health (NIMH) Center for Collaborative Studies of Mental Disorders-funded Rutgers University Cell and DNA Repository (<http://www.rucdr.org/mental-health>) (RUCDR). All cells were cultured under standard conditions (37°C, 5% CO₂, and 100% humidity).

Generation of 2D neuronal cultures. The neural progenitor cells (NPCs) were derived from iPSCs as previously described (28) and cultured in neurobasal medium supplemented with 2% B27 and 10 ng/ml brain-derived neurotrophic factor (BDNF) for 6 weeks. Half of the culture medium was changed every other day.

Generation of 3D neuronal cultures (brain organoids). hiPSCs were cultured in neural progenitor selection medium including dual SMAD inhibitors SB431542 (10 μ M) and LDN193189 (100 nM) (NPS/Dual-SMAD medium). After 4 to 5 days in NPS/Dual-SMAD, neural rosettes (250 to 500 μ m in diameter) were dissected manually and cultured in NPS/Dual-SMAD medium on ultralow attachment plates for another 2 to 3 days. Neural rosettes were then replated to Matrigel-coated plates. After overnight incubation, the aggregates containing 1 to 4 neural rosettes were isolated manually, transferred into 10-cm petri dishes, and cultured in cortical organoid differentiation medium I (Dulbecco's modified essential medium [DMEM]-F12–neurobasal [1:1, vol/vol]) supplemented with 1 \times GlutaMAX, 1 \times B-27 (VitA[–]), 0.5 \times nonessential amino acids, 0.5 \times N-2, insulin (2.5 μ g), and 1 \times penicillin-streptomycin (P/S) on an orbital shaker. One week later, the organoids were transferred into cortical organoid differentiation medium II (DMEM-F12–neurobasal [1:1, vol/vol]) supplemented with 1 \times GlutaMAX, 1 \times B-27 (VitA[+]), 0.5 \times nonessential amino acids, 0.5 \times N-2, insulin (2.5 μ g), BDNF (10 ng/ml), and 1 \times P/S. Culture medium was changed every 3 days.

Early-stage neocortical organoids (day 33) exhibited a mosaic of ventricular zone (VZ)-like structures most of them containing a single central ventricle-like cavity (Fig. 2a). The forebrain identity of the developing organoids was supported by their expression of FOXG1 (Fig. 2b). Neural progenitor cells in the VZ-like structures expressed sex-determining region Y-box 2 (SOX2) (Fig. 2c). Immunostaining for vimentin (a marker of radial glial cells [29]) in the VZ-like regions was also observed (Fig. 2d). The intermediate progenitor cells in the VZ-subventricular zone (SVZ)-like regions were highlighted by the expression of T-box brain protein 2 (TBR2) (Fig. 2e). Cut-like homeobox 2 (Cux2)-immunoreactive neural precursor cells (Fig. 2f), which are found in the SVZ and the intermediate zone during early stages of brain development and differentiate into upper layer neurons, were observed (Fig. 2f). Neuronal differentiation in the cortical organoids is shown by the expression of the neuronal markers neuron-specific class III beta-tubulin (TUJ1) and microtubule-associated protein 2 (MAP2) (Fig. 2f and 3a). Immunohistochemistry for deep cortical layers markers T-box brain protein 1 (TBR1), calbindin, and chicken ovalbumin upstream promoter transcription factor interacting protein 2 (CTIP2) (Fig. 1g to i), and the superficial layers neurons expressing special AT-rich sequence-binding protein 2 (SATB2) (Fig. 1j) were observed. Overall, these results indicate that the organoids employed in this study exhibit architectural features of a developing brain.

Viral infections. HSV-1 strain KOS (VR-1493; ATCC) was employed in this study.

(i) Infection of 2D neuronal cultures. For lytic infections, cell-free virus was adsorbed onto monolayer cultures of hiPSC-derived neurons at a range of multiplicities of infection (MOIs), from 1 to 0.3. One hour after the infection, the inocula were removed, and cells were washed twice with DMEM-F12 medium and cultured with neurobasal medium for 48 h. For latent infections, cells were preincubated with 5BVdU plus IFN- α . After 24 h, cells were infected at an MOI of 0.3 and cultured with neurobasal medium in the presence of 5BVdU and IFN- α for 48 h.

(ii) Infection of brain organoids. Brain organoids were transferred singularly in 1.5-ml Eppendorf tubes and washed with 500 μ l of DMEM-F12 medium. The medium was then discarded, and 50 μ l of neurobasal medium with or without 5BVdU and IFN- α containing 3,000 PFU of HSV-1 was added. After perforating the cap of Eppendorf tubes using a 20-gauge sterile needle, the organoids were cultured in an incubator under standard conditions (5% CO₂, 37°C, and 100% humidity). To inhibit viral replication, the organoids were pretreated with 5BVdU plus IFN- α for 24 h. Two hours after the infection, the inoculum was removed, and the organoids were washed twice with 500 μ l of DMEM-F12 medium and cultured singularly in cortical medium II in the presence or absence of 5BVdU and IFN- α in low-attachment 24-well plates on an orbital shaker. Infected organoids were prepared for immunohistochemistry analysis at days 3 and 5 postinfection.

Immunofluorescence. The 2D neuronal cultures were fixed with 4% paraformaldehyde and permeabilized with 0.2% Triton-X before immunostaining. The paraffin-embedded slices of organoids were prepared as follows. The organoids were rinsed in phosphate-buffered saline (PBS) and fixed by immersing in at least 10 volumes of 10% formalin overnight at 4°C. The organoids were rinsed again and then embedded in blocks of low-melting-point agarose. The agarose blocks were embedded in paraffin wax by following a standard protocol for formalin-fixed tissue and then sectioned to 5 μ m for subsequent staining. Before staining, paraffin sections were incubated at 60°C, dewaxed in xylene, hydrated in absolute, 95%, and 70% ethanol, and rinsed in pure water. Antigen unmasking was performed by exposing

paraffin sections to antigen retrieval Citra solution (Biogenex) at 95°C. Paraffin sections were incubated with SuperBlock blocking buffer (Thermo Scientific) before immunostaining. Paraffin sections were also stained with hematoxylin and eosin reagents.

Samples were incubated with primary antibodies overnight at 4°C. Primary antibodies used were mouse monoclonal anti- β -tubulin III antibody (conjugated clone TUJ1; NL1195V; 1:100 dilution; R&D Systems), mouse monoclonal anti-MAP2 antibody (AB5622, 1:500 dilution; Millipore), rabbit polyclonal anti-calbindin antibody (AB11426, 1:400 dilution; Abcam), rabbit polyclonal anti-vimentin antibody (AB45939, 1:500 dilution; Abcam), rabbit polyclonal anti-CUX-2 antibody (AB130395, dilution 1:200; Abcam), mouse monoclonal anti-HSV-1 ICP4 antibody (AB6514, dilution 1:200; Abcam), rabbit polyclonal anti A β 42 antibody (AB5078P, 1:500 dilution; Millipore), rabbit polyclonal anti-FOXG1 antibody (18259, 1:1,000 dilution; Abcam), rat monoclonal anti-CTIP2 antibody (AB18465, 1:500 dilution; Abcam), rabbit polyclonal anti-TBR1 antibody (AB31940, 1:500 dilution; Abcam), chicken polyclonal anti-TBR2 antibody (AB15894, 1:500 dilution; Millipore), and rabbit polyclonal anti-SATB2 antibody (AB34735, 1:1,000 dilution; Abcam).

The following fluorophore-conjugated secondary antibodies were used to detect bound primary antibodies: Alexa Fluor 488 goat anti-rabbit (1:300 dilution; Thermo Fisher Scientific), Alexa Fluor 488 goat anti-mouse (A-10680, 1:300 dilution; Thermo Fisher Scientific), Alexa Fluor 594 goat anti-rabbit (A-11012, 1:300 dilution; Thermo Fisher Scientific), Alexa Fluor 594 goat anti-mouse secondary antibody (A-11005, 1:300 dilution; Thermo Fisher Scientific), Alexa Fluor 488 goat anti-chicken secondary antibody (A-11039, 1:300 dilution; Thermo Fisher Scientific), and Alexa Fluor 488 goat anti-rat (711-545-152, 1:300 dilution; Jackson ImmunoResearch Labs). A Leica IL MD LED inverted fluorescence microscope was used for image acquisition.

ACKNOWLEDGMENTS

The work in the manuscript was supported in part by the following: Stanley Medical Research Institute (07R-1712), NINDS (R01NS115082 and R21NS096405), NIA (P01AG014449, P01AG025204, and R01AG052528), and the Veterans Health Administration (I01RX000952 and I01RX001778).

The content is solely the responsibility of the authors and does not necessarily represent the official views of the National Institutes of Health, the Department of Veterans Affairs, or the United States Government.

REFERENCES

- Serrano-Pozo A, Frosch MP, Masliah E, Hyman BT. 2011. Neuropathological alterations in Alzheimer disease. *Cold Spring Harb Perspect Med* 1: a006189. <https://doi.org/10.1101/cshperspect.a006189>.
- Choi SH, Kim YH, Hebisch M, Sliwinski C, Lee S, D'Avanzo C, Chen H, Hooli B, Asselin C, Muffat J, Klee JB, Zhang C, Wainger BJ, Peitz M, Kovacs DM, Woolf CJ, Wagner SL, Tanzi RE, Kim DY. 2014. A three-dimensional human neural cell culture model of Alzheimer's disease. *Nature* 515:274–278. <https://doi.org/10.1038/nature13800>.
- McGeer PL, Rogers J, McGeer EG. 2016. Inflammation, antiinflammatory agents, and Alzheimer's disease: the last 22 years. *J Alzheimers Dis* 54:853–857. <https://doi.org/10.3233/JAD-160488>.
- Sperling RA, Aisen PS, Beckett LA, Bennett DA, Craft S, Fagan AM, Iwatsubo T, Jack CR, Kaye J, Montine TJ, Park DC, Reiman EM, Rowe CC, Siemers E, Stern Y, Yaffe K, Carrillo MC, Thies B, Morrison-Bogorad M, Wagster MV, Phelps CH. 2011. Toward defining the preclinical stages of Alzheimer's disease: recommendations from the National Institute on Aging-Alzheimer's Association workgroups on diagnostic guidelines for Alzheimer's disease. *Alzheimers Dement* 7:280–292. <https://doi.org/10.1016/j.jalz.2011.03.003>.
- Selkoe DJ, Hardy J. 2016. The amyloid hypothesis of Alzheimer's disease at 25 years. *EMBO Mol Med* 8:595–608. <https://doi.org/10.15252/emmm.201606210>.
- Alzheimer A, Stelzmann RA, Schnitzlein HN, Murtagh FR. 1995. An English translation of Alzheimer's 1907 paper, "Über eine eigenartige Erkrankung der Hirnrinde." *Clin Anat* 8:429–431. <https://doi.org/10.1002/ca.980080612>.
- Moir RD, Lathe R, Tanzi RE. 2018. The antimicrobial protection hypothesis of Alzheimer's disease. *Alzheimers Dement* 14:1602–1614. <https://doi.org/10.1016/j.jalz.2018.06.3040>.
- Li H, Liu CC, Zheng H, Huang TY. 2018. Amyloid, tau, pathogen infection and antimicrobial protection in Alzheimer's disease-conformist, nonconformist, and realistic prospects for AD pathogenesis. *Transl Neurodegener* 7:34. <https://doi.org/10.1186/s40035-018-0139-3>.
- Wozniak MA, Mee AP, Itzhaki RF. 2009. Herpes simplex virus type 1 DNA is located within Alzheimer's disease amyloid plaques. *J Pathol* 217:131–138. <https://doi.org/10.1002/path.2449>.
- Wozniak MA, Itzhaki RF, Shipley SJ, Dobson CB. 2007. Herpes simplex virus infection causes cellular beta-amyloid accumulation and secretase upregulation. *Neurosci Lett* 429:95–100. <https://doi.org/10.1016/j.neulet.2007.09.077>.
- De Chiara G, Piacentini R, Fabiani M, Mastrodonato A, Marcocci ME, Limongi D, Napoletani G, Protto V, Coluccio P, Celestino I, Li Puma DD, Grassi C, Palamara AT. 2019. Recurrent herpes simplex virus-1 infection induces hallmarks of neurodegeneration and cognitive deficits in mice. *PLoS Pathog* 15:e1007617. <https://doi.org/10.1371/journal.ppat.1007617>.
- Cairns DM, Rouleau N, Parker RN, Walsh KG, Gehrke L, Kaplan DL. 2020. A 3D human brain-like tissue model of herpes-induced Alzheimer's disease. *Sci Adv* 6:eaay8828. <https://doi.org/10.1126/sciadv.aay8828>.
- Eimer WA, Vijaya Kumar DK, Navalpur Shanmugam NK, Rodriguez AS, Mitchell T, Washicosky KJ, György B, Breakefield XO, Tanzi RE, Moir RD. 2018. Alzheimer's disease-associated β -amyloid is rapidly seeded by herpesviridae to protect against brain infection. *Neuron* 100:1527–1532. <https://doi.org/10.1016/j.neuron.2018.11.043>.
- D'Aiuto L, Bloom DC, Naciri JN, Smith A, Edwards TG, McClain L, Callio JA, Jessup M, Wood J, Chowdari K, Demers M, Abrahamson EE, Ikonovic MD, Viggiano L, De Zio R, Watkins S, Kinchington PR, Nimgaonkar VL. 2019. Modeling HSV-1 infections in human CNS neuronal cells using two-dimensional and three-dimensional cultures derived from induced pluripotent stem cells. *J Virol* 93:e00111-19. <https://doi.org/10.1128/JVI.00111-19>.
- Wozniak MA, Frost AL, Preston CM, Itzhaki RF. 2011. Antivirals reduce the formation of key Alzheimer's disease molecules in cell cultures acutely infected with herpes simplex virus type 1. *PLoS One* 6:e25152. <https://doi.org/10.1371/journal.pone.0025152>.
- Little CS, Hammond CJ, MacIntyre A, Balin BJ, Appelt DM. 2004. Chlamydia pneumoniae induces Alzheimer-like amyloid plaques in brains of BALB/c mice. *Neurobiol Aging* 25:419–429. [https://doi.org/10.1016/S0197-4580\(03\)00127-1](https://doi.org/10.1016/S0197-4580(03)00127-1).
- Miklosy J, Kis A, Radenovic A, Miller L, Forro L, Martins R, Reiss K, Darbinian N, Darekar P, Mihaly L, Khalili K. 2006. Beta-amyloid deposition

- and Alzheimer's type changes induced by *Borrelia* spirochetes. *Neurobiol Aging* 27:228–236. <https://doi.org/10.1016/j.neurobiolaging.2005.01.018>.
18. Spitzer P, Condic M, Herrmann M, Oberstein TJ, Scharin-Mehlmann M, Gilbert DF, Friedrich O, Grömer T, Kornhuber J, Lang R, Maler JM. 2016. Amyloidogenic amyloid- β -peptide variants induce microbial agglutination and exert antimicrobial activity. *Sci Rep* 6:32228. <https://doi.org/10.1038/srep32228>.
 19. Soscia SJ, Kirby JE, Washicosky KJ, Tucker SM, Ingelsson M, Hyman B, Burton MA, Goldstein LE, Duong S, Tanzi RE, Moir RD. 2010. The Alzheimer's disease-associated amyloid beta-protein is an antimicrobial peptide. *PLoS One* 5:e9505. <https://doi.org/10.1371/journal.pone.0009505>.
 20. White MR, Kandel R, Tripathi S, Condon D, Qi L, Taubenberger J, Hartshorn KL. 2014. Alzheimer's associated β -amyloid protein inhibits influenza A virus and modulates viral interactions with phagocytes. *PLoS One* 9:e101364. <https://doi.org/10.1371/journal.pone.0101364>.
 21. Piacentini R, Civitelli L, Ripoli C, Marcocci ME, De Chiara G, Garaci E, Azzena GB, Palamara AT, Grassi C. 2011. HSV-1 promotes Ca²⁺-mediated APP phosphorylation and A β accumulation in rat cortical neurons. *Neurobiol Aging* 32:e13–e26. <https://doi.org/10.1016/j.neurobiolaging.2010.06.009>.
 22. Piacentini R, Li Puma DD, Ripoli C, Marcocci ME, De Chiara G, Garaci E, Palamara AT, Grassi C. 2015. Herpes simplex virus type-1 infection induces synaptic dysfunction in cultured cortical neurons via GSK-3 activation and intraneuronal amyloid- β protein accumulation. *Sci Rep* 5:15444. <https://doi.org/10.1038/srep15444>.
 23. Powell-Doherty RD, Abbott ARN, Nelson LA, Bertke AS. 2020. Amyloid- β and p-Tau anti-threat response to herpes simplex virus 1 infection in primary adult murine hippocampal neurons. *J Virol* 94:e01874–19. <https://doi.org/10.1128/JVI.01874-19>.
 24. Li Puma DD, Piacentini R, Leone L, Gironi K, Marcocci ME, De Chiara G, Palamara AT, Grassi C. 2019. Herpes simplex virus type-1 infection impairs adult hippocampal neurogenesis via amyloid- β protein accumulation. *Stem Cells* 37:1467–1480. <https://doi.org/10.1002/stem.3072>.
 25. Abbott A. 2003. Cell culture: biology's new dimension. *Nature* 424:870–872. <https://doi.org/10.1038/424870a>.
 26. Drayman N, Patel P, Vistain L, Tay S. 2019. HSV-1 single-cell analysis reveals the activation of anti-viral and developmental programs in distinct sub-populations. *Elife* 8:e46339. <https://doi.org/10.7554/eLife.46339>.
 27. Tzeng NS, Chung CH, Lin FH, Chiang CP, Yeh CB, Huang SY, Lu RB, Chang HA, Kao YC, Yeh HW, Chiang WS, Chou YC, Tsao CH, Wu YF, Chien WC. 2018. Anti-herpetic medications and reduced risk of dementia in patients with herpes simplex virus infections—a nationwide, population-based cohort study in Taiwan. *Neurotherapeutics* 15:417–429. <https://doi.org/10.1007/s13311-018-0611-x>.
 28. D'Aiuto L, Zhi Y, Kumar Das D, Wilcox MR, Johnson JW, McClain L, MacDonald ML, Di Maio R, Schurdak ME, Piazza P, Viggiano L, Sweet R, Kinchington PR, Bhattacharjee AG, Yolken R, Nimgaonka VL, Nimgaonkar VL. 2014. Large-scale generation of human iPSC-derived neural stem cells/early neural progenitor cells and their neuronal differentiation. *Organogenesis* 10:365–377. <https://doi.org/10.1080/15476278.2015.1011921>.
 29. Vinci L, Ravarino A, Fanos V, Naccarato AG, Senes G, Gerosa C, Bevilacqua G, Faa G, Ambu R. 2016. Immunohistochemical markers of neural progenitor cells in the early embryonic human cerebral cortex. *Eur J Histochem* 60:2563. <https://doi.org/10.4081/ejh.2016.2563>.